Supplemental Information

Surface Modified Materials for Active Capture of Enzymes

Dandan Wang[1], William Hartz[2], Mark G. Moloney[1,2]*

[1]Oxford Suzhou Centre for Advanced Research, Building A, 388 Ruo Shui Road,

Suzhou Industrial Park, Jiangsu, 215123, P.R. China

[2]Chemistry Research Laboratory, Department of Chemistry, University of Oxford, Oxford OX1

3TA, U.K.

*mark.moloney@chem.ox.ac.uk

1. Synthetic procedure of bis(diaryldiazomethane) and spacer

Synthesis of 1,3-bis(diazo(4-phenoxyphenyl)methyl)benzene was adapted from work done previously and Figure S1 shows the synthetic route.[1] Synthetic route of spacer was shown in Figure S2, and the detailed procedure can be found in previous report.[2]
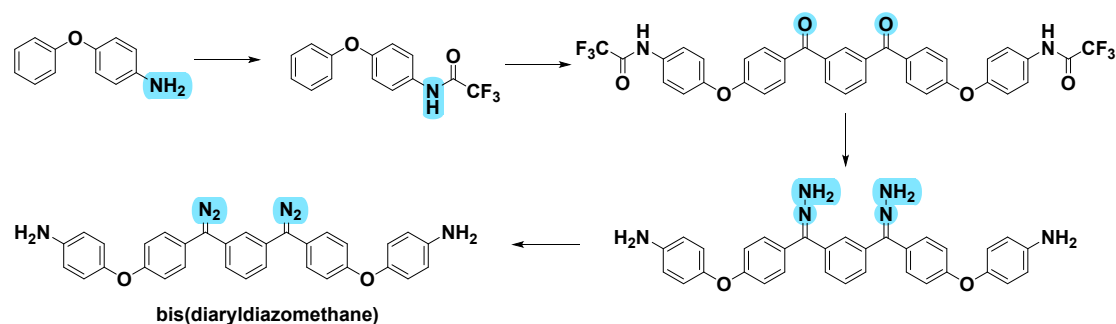

Figure S1. synthetic route for 1,3-bis(diazo(4-phenoxyphenyl)methyl)benzene.
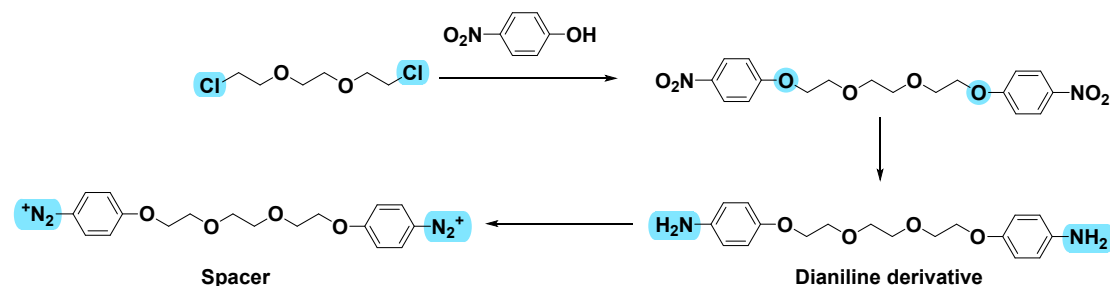
Figure S2. synthetic route for dianiline derivative and spacer.

2. Surface modification procedure

In this study, five different materials-XAD4 (polystyrene bead), MAC3 (polyacrylate bead), glass wool, glass fiber (GF) membrane, and PTFE membrane-were selected for surface modification. They are all commercially available, either in bead or fiber form, and our modification approach utilized previous reported methodology.[1,2]

2.1 S-carbene-NH$_2$ formation

The bis(diaryldiazomethane) was fully dissolved in DCM (20 mg/mL), the material **S** (For support **S** = XAD4, MAC3 and glass wool, 400 mg support was immersed in 5 mL DCM, for support **S** =

GF membrane and PTFE membrane, 1 piece was immersed in 1 mL DCM) was added to the solution and DCM was evaporated slowly and with care in vacuo. The resulting mixture was then heated at 120 °C for 30 min unsealed. A change in color of the material indicated a successful surface modification. The material was then washed with a copious amount of DCM until no colour was seen to be washed out and were dried in a sintered funnel to yield the carbene modified surface **S-carbene-NH$_2$.**

2.2 S-carbene-N$_2^+$ formation

S-carbene-NH$_2$ (100 mg or 1 piece for membrane) was added in a conical flask, 0.5 mL ethanol was added, and the mixture was cooled with ice/water bath. Add HCl (63.5 μL 3M) into the flask and left for 1.5 hr whilst occasionally swirling the vial. NaNO$_2$ (8 mg) was dissolved in water (0.25 mL) and added to the cooled mixture. The flask was then left to stand for 4 hr whilst occasionally swirling. The diazonium surface **S-carbene-N$_2^+$** was then used *in situ* immediately.

2.3 S-carbene-spacer-N$_2^+$ formation

To a 4 mL ethanol/water (1:1) mixture, dianiline derivative (4,4'-(((ethane-1,2-diylbis(oxy))bis(ethane-2,1-diyl))bis(oxy))dianiline) (83 mg, 0.25 mmol, 1 eq) was added and cooled with ice/water bath. HCl (0.67 mL, 3M) was added and stirred for 5 min, NaNO$_2$ (75.9 mg, 2.2 eq) in 2 mL H$_2$O was added and stirred for 30 min, meanwhile, the reaction mixture turned to purple. 2 mL reaction mixture was taken out and directly added into a conical flask with M-carbene-NH$_2$ (100 mg or one piece for membrane). The mixture was then left to stand for 18 hr whilst occasionally swirling and the diazonium surface **S-carbene-spacer-N$_2^+$** used *in situ* for enzyme immobilization.

3. Surface energy results

Surface energy for immobilized enzyme surface was studied. Contact angle went zero quickly using both water and diiodomethane, so the contact angle was taken when the liquid was first in contact with surface. For membrane, the contact angle was a balance between porosity and surface chemical properties, so the relation between w and surface energy was not straightforward.

Table S1. contact angle and surface energy for immobilized cellulase surface for modified

Membrane	θ_{H_2O} (°)	θ_{DIM} (°)	γ_S (mN/m)	γ_S^D (mN/m)	γ_S^P (mN/m)
GF-cellulase	17.1±2.8	25.8±1.4	73.0±1.8	9.2±0.3	63.8±1.5
GF-carbene-N=N-cellulase-5 mg	65.6±12.5	26.8±12.1	36.9±15.4	15.7±3.8	21.3±11.6
GF-carbene-N=N-cellulase-20 mg	52.5±7.9	20.2±11.3	47.1±10.3	14.2±2.3	32.9±8.0
GF-carbene-N=N-cellulase-50 mg	71.6±4.9	27.2±2.5	33.1±5.9	17.0±1.2	16.1±4.2

4. XPS for GF membrane series

XPS measurement of different glass membrane surfaces with $w = 20$ mg/mL were compared, with the full scans and narrow scans of C 1s, N 1s, O 1s, Si 2p and S 2p shown in Figure S3. An ~0.5 eV shift of the Si 2p peak was observed when the bare GF membrane was modified with bis(diarylcarbene), as shown in Figure S3e, the drastic decrease of Si 2p peak indicating the embedding of Si with bis(diarycarbene) molecules. After further modification with spacer or enzyme immobilization, Si 2p signal gradually vanished. Peak deconvolution of C 1s and N 1s spectra was done with Thermo advantage software and a calculation of the deconvoluted peaks were summarized in Table S2 and Table S3.
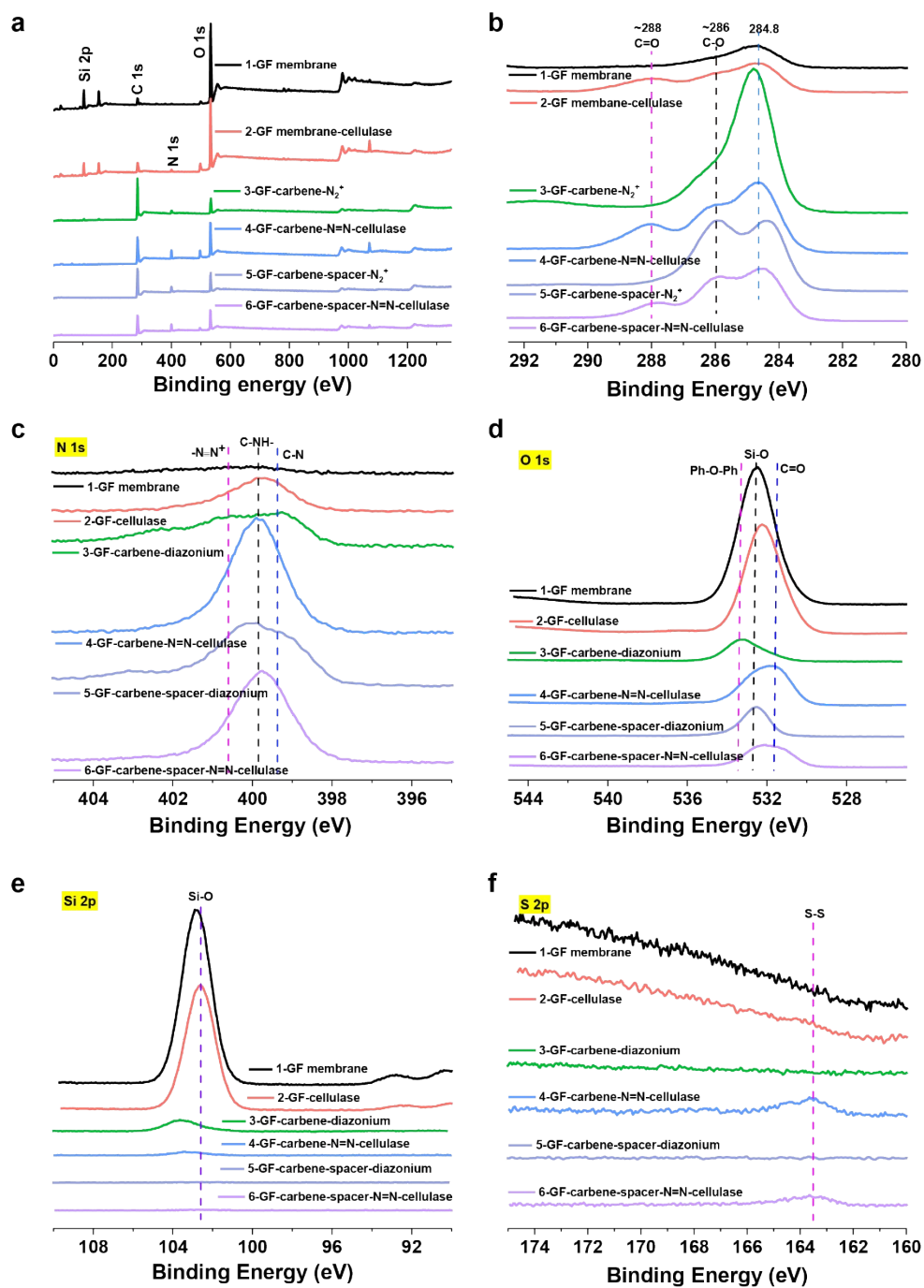
Figure S3. Full scan and High resolution C1s, N 1s, O 1s, Si 2p and S 2p XPS spectra for surfaces of GF membrane series.

Table S2. Surface elemental (atom%) components determined by high resolution C 1s spectra after peak deconvolution.

Surface information	After deconvolution (atom%)			C-O/C-C
	C-C	C-O	C=O	
GF membrane	5.8	5.12	0.44	0.882759

GF membrane-cellulase	10.6	5.53	6.95	0.521698
GF-carbene-N_2^+	62.72	16.46	0	0.262436
GF-carbene-N=N-cellulase	30.39	18.63	13.73	0.613031
GF-carbene-spacer-N_2^+	28.64	45.86	0	1.601257
GF-carbene-spacer-N=N-cellulase	31.38	26.39	10.36	0.840982

Table S3. Surface elemental (atom%) components determined by high resolution N 1s spectra after peak deconvolution.

Surface information	After deconvolution (atom%)		N=N/NH
	-NH-	-N=N-	
GF-cellulase	0.38	0	0
GF-carbene-N=N-cellulase-5 mg	10.52	3.48	0.33
GF-carbene-N=N-cellulase-20 mg	9.29	7.28	0.78
GF-carbene-N=N-cellulase-20 mg	11.66	4.02	0.34

5. Surface morphology comparison of cellulase on GF modified membrane at different concentration *w*

The surface morphology of bis(diarylcarbene) modified GF membrane at different *w* had been reported in previous literature.[2] As can be seen from the SEM images in Figure S4, as the concentration *w* increases from 0 to 50 mg/mL, more fibers are welded by film joints due to polymerization and cross-linking of bis(diarycarbene) for both **GF-carbene-N=N-cellulase** and **GF-carbene-spacer-cellulase**. The attachment of cellulase does not change the connection but make the surface rougher with aggerated cellulase observed at higher magnification indicated in the main text. **Note**: each SEM image is obtained from an individual piece membrane, the area spotted for SEM imaging is randomly selected, and the morphology at the same concentration of *w* may look different is due to the non-uniformity of the membrane in microscale, but the trend of w increasing from 0 to 50 mg/mL was comparable.
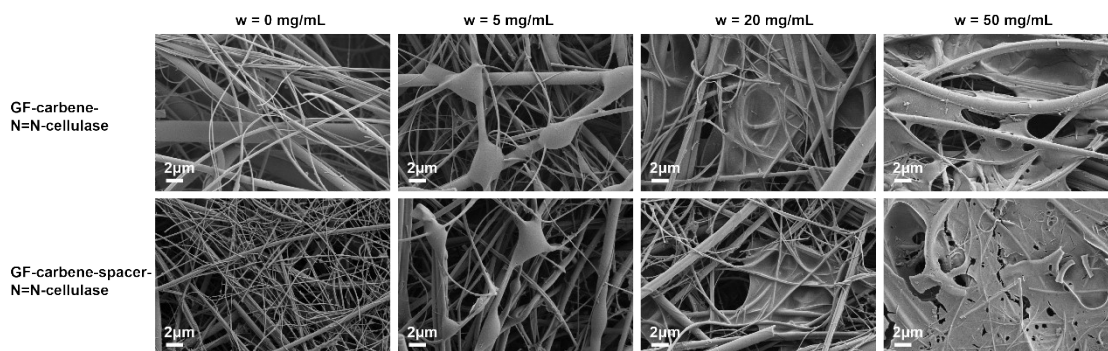
Figure S4. SEM images of cellulase on modified GF membrane at w = 0, 5, 20 and 50 mg/mL.

6. Immobilized enzyme properties

As shown in Figure S5a, the pristine XAD4 beads gave the highest enzyme loading, while the modified ones exhibited significantly lower loading. This may be attributed to the higher surface area of pristine XAD4 (864.6 m^2/g, see Table S4) than that of modified beads (526.8 m^2/g for **XAD4-carbene-NH$_2$**), for which pores become blocked or narrowed by the crosslinking carbene. MAC3 beads also showed a similar trend as that of XAD4, with highest enzyme loading on unmodified beads. While BET analysis shows the surface area of pristine MAC3 beads (18.2 m^2/g, Table S4) is much lower than that of XAD4, the enzyme loading capacity by using MAC3 beads is around 7 times higher than that by XAD4, and the most likely reason is that the carboxyl groups on the MAC3 surface allow for strong non-covalent interactions (i.e., hydrogen bonding and electrostatic interactions) with cellulase enhancing the enzyme adsorption. Since XAD4 and MAC3 are both in bead format, their trend for enzyme loading on changing from pristine to modified forms without and with spacer are the same.

For glass wool, GF and PTFE membrane, the highest loading capacity is for **S-carbene-N$_2$**$^+$; these materials are fibrous, probably enabling better contact of enzyme with diazonium salt during

immobilization, and facilitating the azo coupling reaction, with the highest loading obtained for modified GF membrane.

The immobilized enzyme activity was shown in Figure S5b, for XAD4, although the enzyme loading on the beads is the lowest compared to other materials, very high activity for the supported material with spacer (**S-carbene-spacer-N$_2$$^+$**) was found. The trend in Figure S5b clearly shows that covalently bonded cellulase has a higher activity than physisorbed cellulase, which is probably due to the decrease in steric hinderance for the substrate-cellulase interaction, allowing better diffusion. For MAC3, the trend in cellulase activity is opposite to their loading capacity, so that the higher loading of cellulase on the support surface leads to a higher probability of conformational change induced by strong non-covalent interaction[3] or non-accessibility of enzyme by overlapping and aggregation.
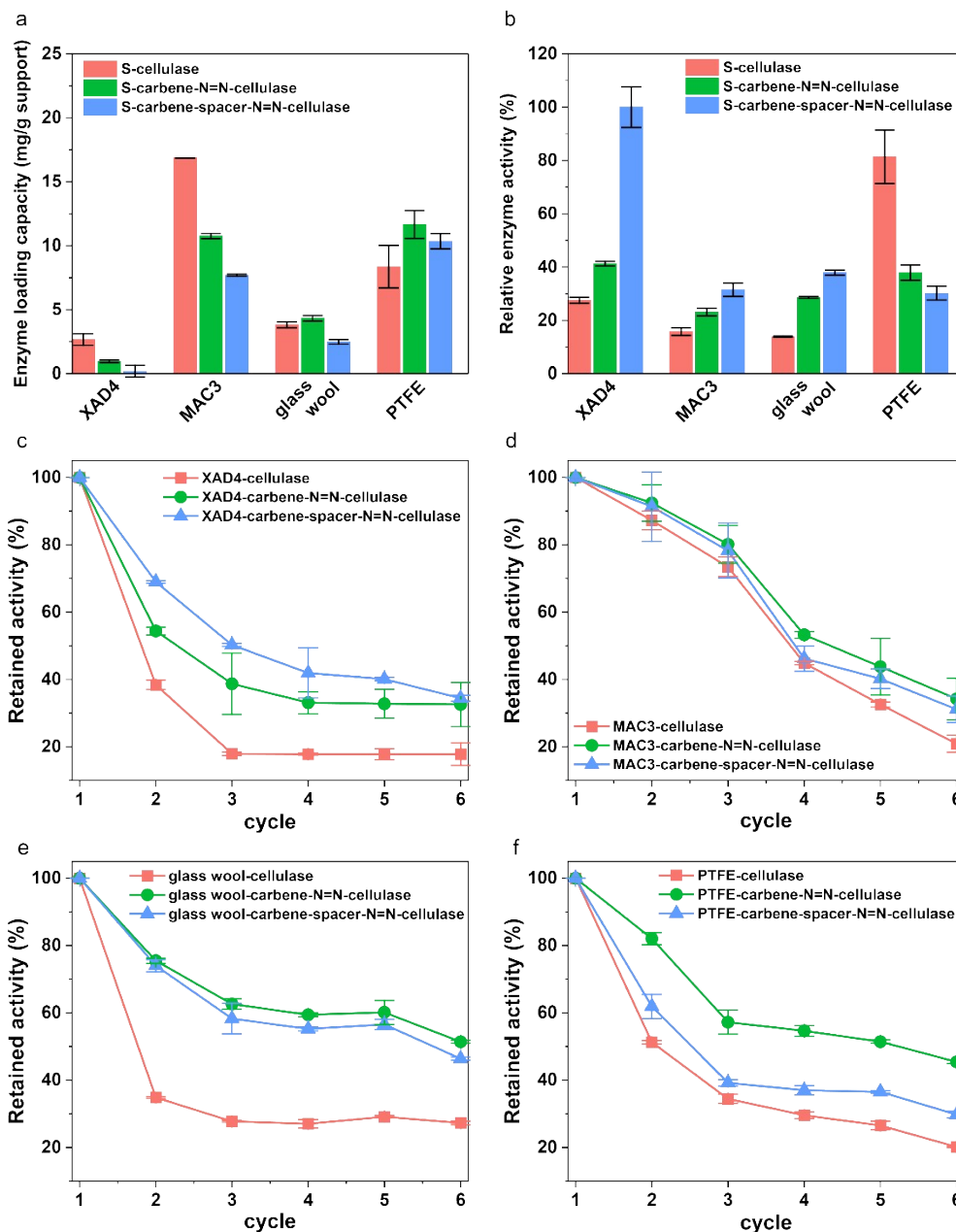
Figure S5. Histograms of a) enzyme loading capacity for different supports; b) relative enzyme activity on different supports; Reusability plot of cellulase on c) XAD4 and modified surface; d) MAC3 and modified surface; e) glass wool and modified surface; f) PTFE membrane and modified surface. (50 $^{\circ}$C, 50 μM acetate buffer, pH 4.8, 30 min).

The BET surface area was calculated from the BET plot, due to the solidity of glass wool, glass fiber membrane and PTFE membrane, its BET surface area was lower than 10 m^2/g.

Table S4. BET surface area data of bare materials.

Materials	XAD4	MAC3	Glass wool	GF membrane	PTFE membrane
Surface area(m²/g)	864.6	18.2	6.8	2.4	2.9

Confirmation of cellulase on surface was also down by direct treating membrane with Bradford agent. As demonstrated in Figure S6, membrane with cellulase has obvious color change   after adding Bradford agent. However, this experiment only proved the existence of cellulase on surface but not covalent bonding of cellulase on surface.
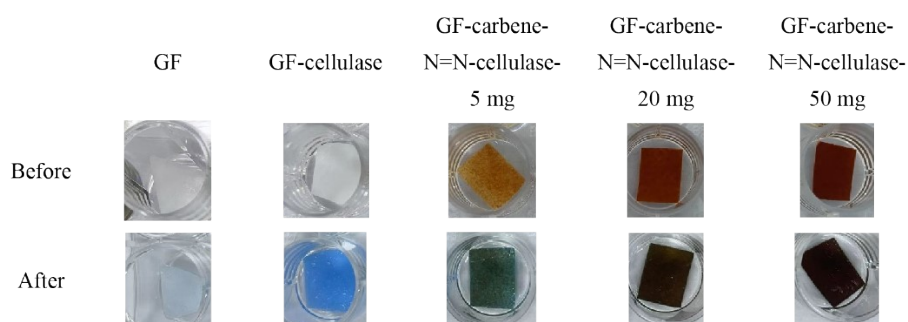
Figure S6. Membrane before and after reaction with Bradford agent for 10 min.

7.   Comparison of current work with previous reports

Here, Table S5 summarizes the recent reports related to covalent bonding with cellulase. It should be noted that to judge the effectiveness of a method, specific conditions like support availability, type, covalent binding agent, cellulase loading, retained activity and reusability should all be taken into consideration. For example, the retained activity in our work is lower compared with these lab-prepared nano and micromaterials, which is to be expected since they provide much higher surface area. Compared with other commercial materials in Table S5, although our retained activity is not

the highest, its reusability is the best. Furthermore, compared with commonly used glutaraldehyde, covalent binding via diazonium is not commonly used but diazonium can specifically bind with tyrosine groups and does not need lysine residues as required for glutaraldehyde linking.

In addition, the use of glass material as a support for enzyme immobilization is summarized in Table S6. In these papers, adsorption was the major technique for enzyme immobilization, while for covalent binding, silanization followed by glutaraldehyde was the process commonly used. Bisdiarylcarbene modified glass fiber proved to be a good support compared with other modified or unmodified glass material with high enzyme loading and reusability, and with a fully novel immobilization mechanism.

Table S5. Supports, covalent bonding agent, cellulase loading, activity and reusability summary of current work and other report.

No.	Support type	support	availability	covalent binding	cellulase loading	Retained activity	reusability	ref
1	membrane	**GF membrane**	**Commercial (recyclable)**	**bis(diarylcarbene)**	**23 mg/g support**	**40%**	**91% after 6 cycles**	**This work**
2		poly(vinyl alcohol) PVA membrane	commercial	glutaraldehyde	11.4% (efficiency)	65%	36% after 6 cycles	4
3		polyacrylonitrile (PAN) membrane	commercial	amidination	30 mg/g support	64%	40% after 5 cycles	5
4		acrylamide grafted PAN membranes	Lab prepared	glutaraldehyde	35.22%	22.1%	NA	6
5	Nano and micro materials	graphene oxide	lab prepared	P-β-sulfuric acid ester ethyl sulfone aniline (SESA)	4.6 mg/g support	90%	80% after 9 cycles	7
6		Polyurea (PU) microsphere	lab prepared	glutaraldehyde	39.2 mg/g support	77.90%	80% after 8 cycles	8
7		Fe_3O_4 nanoparticles	lab prepared	epoxy polymer	106.1 mg/g support	NA	60% after 6 cycles	9
8		silica gel	commercial	APTES and glutaraldehyde	18.8 mg/g support	7%	60% after 10 cycles	10
9		MTEP (terpolymers and Fe_3O_4)	lab prepared	epoxy	18.36 mg/g support	48.20%	51.3% after 6 cycles	11
10		Magnetic Halloysite Nanotubes	lab prepared	APTES and glutaraldehyde	111.6 mg/g support	93.50%	53% after 7 cycles	12

11		MWCNTs	lab prepared	EDC and NHS	22.61 U/mL	98%	NA	13
12		Fe_3O_4-NH_2@4-arm-PEG-NH_2	lab prepared	glutaraldehyde	132 mg/g support	82%	50% after 6 cycles	14
13		Fe_3O_4@SiO_2–graphene oxide	lab prepared	Glutaraldehyde	92% (efficiency)	85%	80% after 7 cycles	15
14		Fe_3O_4@SiO_2@p(NIPAM-co-GMA)	lab prepared	Epoxy	233 mg/g support	NA	65.6% after 6 cycles	16
15		Fe_3O_4/GO/CS	lab prepared	Glutaraldehyde	NA	78%	49% after 8 cycles	17
16		GO@Fe_3O_4@4arm PEG NH_2	lab prepared	Glutaraldehyde	575 mg/g support	NA	45% after 8 cycles	18
17		Magnetic coal fly ash (MCFA)-chitosan	lab prepared	Glutaraldehyde	85.8 mg/g support	76.6%	69.9% after 10 cycles	19
18		cellulase/CS/Fe_3O_4	lab prepared	Glutaraldehyde	202.63 mg/g support	NA	52.2% after 15 cycles	20
19		clay–poly(glycidyl methacrylate) composite	lab prepared	Glutaraldehyde	32.7 mg/g support	73.2%	97% after 10 cycles	21
20		magnetic modified chitosan (MCTS)	lab prepared	Glutaraldehyde	94.5% (effiency)	NA	90 mg/kg after 50 cycles	22
21		UiO-66-NH_2	lab prepared	Glutaraldehyde	126.2 mg/g support	63.6%	70% after 5 cycles	23
22	Other	Biochar and chitosan (C@CS)	lab prepared	Glutaraldehyde	94.7%	67%	90.8% after 8 cycles	24
23		Kaolin	commercial	APTES and glutaraldehyde	NA	58%	80% after 8 cycles	25
24		Poly(GMA-co-EDMA)	lab prepared	Glutaraldehyde	NA	65%	18% after 4 cycles	26

| No.	support	Immobilization technique	Binding agent	enzyme	Enzyme loading	Retained activity	reusability	storage	ref
	particle								
25	Polymer beads (PS, PP, PE)	commercial	Photo linker FNAB		NA	NA		90% after 8 cycles	27

Table S6. Current work and previous reports summary using glass materials as support for enzyme immobilization.

No.	support	Immobilization technique	Binding agent	enzyme	Enzyme loading	Retained activity	reusability	storage	ref
1	**Glass fiber membrane**	**covalent**	**Bisdiarylcarbene**	**cellulase**	**23 mg/g support**	**40%**	**91% after 6 cycles**	**NA**	**This work**
2	Glass fiber membrane disc	entrapment	Glutaraldehyde	halohydrin dehalogenase	0.2 mg/g support	62.7%	NA	67% after 60 days at 4°C	28
3	Glass fiber membrane	adsorption	NA	wheat esterase	4.43 mg/membrane	30%	NA	91.1% after 12 days at 4°C	29
4	Glass fiber membrane	covalent	glutaraldehyde or diazotization	trypsin	NA	16700 U/mL	NA	~10000 U/mL after 10 days	30,31
5	glass-pH-electrode	adsorption or entrapment	NA	urease	NA	70%-90%	NA	85%-90% after 4 days	32
6	Porous glass bead	adsorption		D-Amino acid oxidase	500 U/g carrier	0.25 U/mL	NA	NA	33
7	porous glass	covalent	glutaraldehyde	dextranase	NA	NA	NA	63% after 2 weeks	34

8. Kinetic and Thermal stability test for GF membrane series

The kinetic parameters for the GF membrane series were calculated from a double reciprocal plot as elaborated in Figure S7 and given in Table S7. K_m is the CMC (carboxymethylcellulose) concentration when the reaction velocity is half of V_{max}, indicating the affinity of enzyme to substrate. V_{max} is the maximum reaction velocity when cellulase is saturated with CMC substrate and it can be constrained by a diffusion effect.

For physically adsorbed cellulase, K_m values were lower than free cellulase, which indicates higher enzyme affinity to substrate[24,35] showing dispersed cellulase on surface for catalysis. For covalently bonded cellulase, K_m values were higher than that of free cellulase, which indicates lower enzyme affinity for its substrate, unsurprisingly suggesting conformational change or other steric modification of cellulase after covalent bonding.[36,37] The higher V_{max} shows that there are more available active centers of enzyme. This result also shows that after adding spacer between enzyme and support, the affinity of immobilized enzyme to its substrate is improved.
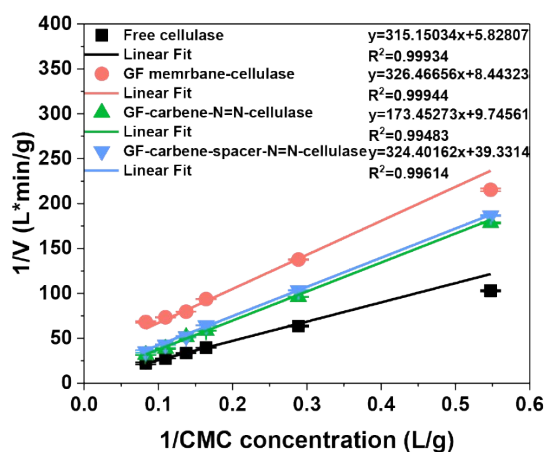

Figure S7. Lineweaver-Burk plot of free and immobilized cellulase.

Table S7. Kinetic parameters for free and immobilized cellulase at reaction temperature 50°C and pH of 4.8.

Enzyme/immobilized enzyme	K_m (g/L)	V_{max} (g/L/min)

Free cellulase	17.80±3.98	0.10±0.02
GF-carbene-N=N-cellulase	54.07±11.44	0.17±0.03
GF-carbene-spacer-N=N-cellulase	38.67±5.43	0.12±0.02
GF-cellulase	8.25±0.76	0.025±0.002

The thermal stability for immobilized cellulase on GF membrane was very similar to that of free cellulase as illustrated in Figure S8, and that implies the interaction between immobilized cellulase and glass fiber membrane surface cannot prevent the conformational changes of cellulase structure at long high temperature exposure. However, our reusability results suggest that, recycle the GF-carbene-cellulase after each 30 min, the retained activity of immobilized cellulase is still high. This gives us an instruction for future experiments and applications.
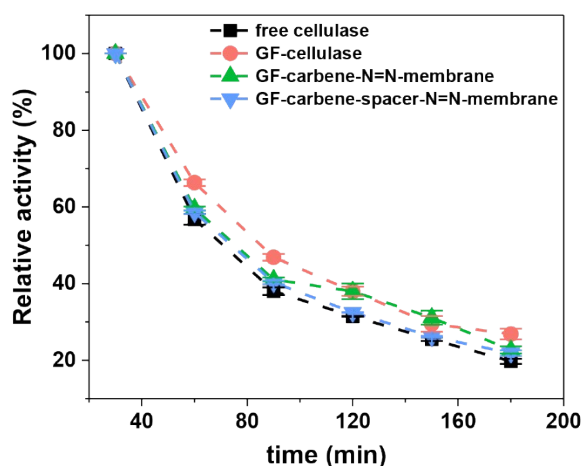
Figure S8. Thermal stability at 50°C, pH 4.8 acetate buffer.

Reference
1.   Moloney, M. G.; Yang, P., Surface Modification of Polymers with Bis(arylcarbene)s from Bis(aryldiazomethane)s: Preparation, Dyeing and Characterization. *RSC Adv.* **2016,** *6*, 111276.
2.   Wang, D.;   Hartz, W.;   Christensen, K. E.; Moloney, M. G., Surface Modification of Glass Fiber Membrane via insertion of a bis(diarylcarbene) assisted with polymerization and cross-linking reactions. *Surf. Interfaces* **2022**, 102155.
3.   Zhang, J.;   Zhang, F.;   Yang, H.;   Huang, X.;   Liu, H.;   Zhang, J.; Guo, S., Graphene oxide as a matrix for enzyme immobilization. *Langmuir* **2010,** *26* (9), 6083-5.

4. Wu, L.; Yuan, X.; Sheng, J., Immobilization of cellulase in nanofibrous PVA membranes by electrospinning. *J. Membr. Sci.* **2005,** *250* (1-2), 167-173.

5. Hung, T. C.; Fu, C. C.; Su, C. H.; Chen, J. Y.; Wu, W. T.; Lin, Y. S., Immobilization of cellulase onto electrospun polyacrylonitrile (PAN) nanofibrous membranes and its application to the reducing sugar production from microalgae. *Enzyme Microb. Technol.* **2011,** *49* (1), 30-7.

6. Yuan, X.-y.; Shen, N.-x.; Sheng, J.; Wei, X., Immobilization of cellulase using acrylamide grafted acrylonitrile copolymer membranes. *J. Membr. Sci.* **1999,** *155* (1), 101-106.

7. Gao, J.; Lu, C.-L.; Wang, Y.; Wang, S.-S.; Shen, J.-J.; Zhang, J.-X.; Zhang, Y.-W., Rapid Immobilization of Cellulase onto Graphene Oxide with a Hydrophobic Spacer. *Catalysts* **2018,** *8* (5), 180.

8. Sui, Y.; Cui, Y.; Xia, G.; Peng, X.; Yuan, G.; Sun, G., A facile route to preparation of immobilized cellulase on polyurea microspheres for improving catalytic activity and stability. *Process Biochem.* **2019,** *87*, 73-82.

9. Hosseini, S. H.; Hosseini, S. A.; Zohreh, N.; Yaghoubi, M.; Pourjavadi, A., Covalent Immobilization of Cellulase Using Magnetic Poly(ionic liquid) Support: Improvement of the Enzyme Activity and Stability. *J. Agric. Food Chem.* **2018,** *66* (4), 789-798.

10. Zhang, D.; Hegab, H. E.; Lvov, Y.; Dale Snow, L.; Palmer, J., Immobilization of cellulase on a silica gel substrate modified using a 3-APTES self-assembled monolayer. *Springerplus* **2016,** *5*, 8.

11. Qi, H.; Duan, H.; Wang, X.; Meng, X.; Yin, X.; Ma, L., Preparation of magnetic porous terpolymer and its application in cellulase immobilization. *Polymer Engineering & Science* **2015,** *55* (5), 1039-1045.

12. Sillu, D.; Agnihotri, S., Cellulase Immobilization onto Magnetic Halloysite Nanotubes: Enhanced Enzyme Activity and Stability with High Cellulose Saccharification. *ACS Sustainable Chem. Eng.* **2019,** *8* (2), 900-913.

13. Alkhatib, M., Statistical modelling optimisation of cellulase enzyme immobilisation on functionalised multi-walled carbon nanotubes for empty fruit bunches degradation. *Australian Journal of Basic and Applied Sciences* **2012,** *6*, 30-38.

14. Han, J.; Wang, L.; Wang, Y.; Dong, J.; Tang, X.; Ni, L.; Wang, L., Preparation and characterization of Fe3O4-NH2@4-arm-PEG-NH2, a novel magnetic four-arm polymer-nanoparticle composite for cellulase immobilization. *Biochem. Eng. J.* **2018,** *130*, 90-98.

15. Li, Y.; Wang, X.-Y.; Jiang, X.-P.; Ye, J.-J.; Zhang, Y.-W.; Zhang, X.-Y., Fabrication of graphene oxide decorated with Fe3O4@SiO2 for immobilization of cellulase. *J. Nanopart. Res.* **2015,** *17* (1), 8.

16. Han, J.; Rong, J.; Wang, Y.; Liu, Q.; Tang, X.; Li, C.; Ni, L., Immobilization of cellulase on thermo-sensitive magnetic microspheres: improved stability and reproducibility. *Bioprocess Biosyst. Eng.* **2018,** *41* (7), 1051-1060.

17. Asar, M. F.; Ahmad, N.; Husain, Q., Chitosan modified Fe3O4/graphene oxide nanocomposite as a support for high yield and stable immobilization of cellulase: its application in the saccharification of microcrystalline cellulose. *Prep Biochem Biotechnol* **2020,** *50* (5), 460-467.

18. Han, J.; Luo, P.; Wang, Y.; Wang, L.; Li, C.; Zhang, W.; Dong, J.; Ni, L., The development of nanobiocatalysis via the immobilization of cellulase on composite magnetic nanomaterial for enhanced loading capacity and catalytic activity. *Int. J. Biol. Macromol.* **2018,** *119*, 692-700.

19. Zang, L.; Qiao, X.; Hu, L.; Yang, C.; Liu, Q.; Wei, C.; Qiu, J.; Mo, H.; Song, G.; Yang, J.; Liu, C., Preparation and Evaluation of Coal Fly Ash/Chitosan Composites as Magnetic Supports for Highly Efficient Cellulase Immobilization and Cellulose Bioconversion. *Polymers* **2018,** *10* (5), 523.

20. Tan, L.; Tan, Z.; Feng, H.; Qiu, J., Cellulose as a template to fabricate a cellulase-immobilized composite with high bioactivity and reusability. *New J. Chem.* **2018,** *42* (3), 1665-1672.

21. Bayramoglu, G.; Senkal, B. F.; Arica, M. Y., Preparation of clay–poly(glycidyl methacrylate) composite support for immobilization of cellulase. *Applied Clay Science* **2013,** *85*, 88-95.

22. Yuan, B.; Yang, X. Q.; Xue, L. W.; Feng, Y. N.; Jiang, J. H., A novel recycling system for nano-magnetic molecular imprinting immobilised cellulases: Synergistic recovery of anthocyanin from fruit and vegetable waste. *Bioresour. Technol.* **2016,** *222*, 14-23.

23. Qi, B.; Luo, J.; Wan, Y., Immobilization of cellulase on a core-shell structured metal-organic framework composites: Better inhibitors tolerance and easier recycling. *Bioresour. Technol.* **2018,** *268*, 577-582.

24. Mo, H.; Qiu, J.; Yang, C.; Zang, L.; Sakai, E.; Chen, J., Porous biochar/chitosan composites for high performance cellulase immobilization by glutaraldehyde. *Enzyme Microb. Technol.* **2020,** *138*, 109561.

25. de Souza Lima, J.; Costa, F. N.; Bastistella, M. A.; de Araujo, P. H. H.; de Oliveira, D., Functionalized kaolin as support for endoglucanase immobilization. *Bioprocess Biosyst. Eng.* **2019,** *42* (7), 1165-1173.

26. Chan, Y. W.; Acquah, C.; Obeng, E. M.; Dullah, E. C.; Jeevanandam, J.; Ongkudon, C. M., Parametric study of immobilized cellulase-polymethacrylate particle for the hydrolysis of carboxymethyl cellulose. *Biochimie* **2019,** *157*, 204-212.

27. Ahirwar, R.; Sharma, J. G.; Nahar, P.; Kumar, S., Immobilization studies of cellulase on three engineered polymer surfaces. *Biocatal. Agric. Biotechnol.* **2017,** *11*, 248-251.

28. Gul, I.; Wang, Q.; Jiang, Q.; Fang, R.; Tang, L., Enzyme immobilization on glass fiber membrane for detection of halogenated compounds. *Anal. Biochem.* **2020,** *609*, 113971.

29. Ye, L.; Liu, X.; Shen, G. H.; Li, S. S.; Luo, Q. Y.; Wu, H. J.; Chen, A. J.; Liu, X. Y.; Li, M. L.; Pu, B.; Qin, W.; Zhang, Z. Q., Properties comparison

between free and immobilized wheat esterase using glass fiber film. *Int. J. Biol. Macromol.* **2019,** *125*, 87-91.

30. Ruckenstein, E.; Guo, W., Cellulose and Glass Fiber Affinity Membranes for the Chromatographic Separation of Biomolecules. *Biotechnol. Prog.* **2004,** *20* (1), 13-25.

31. Guo, W.; Ruckenstein, E., Crosslinked glass fiber affinity membrane chromatography and its application to fibronectin separation. *J. Chromatogr. B* **2003,** *795* (1), 61-72.

32. Sahney, R.; Anand, S.; Puri, B. K.; Srivastava, A. K., A comparative study of immobilization techniques for urease on glass-pH-electrode and its application in urea detection in blood serum. *Anal. Chim. Acta* **2006,** *578* (2), 156-61.

33. Bolivar, J. M.; Nidetzky, B., Oriented and selective enzyme immobilization on functionalized silica carrier using the cationic binding module Z basic2: design of a heterogeneous D-amino acid oxidase catalyst on porous glass. *Biotechnol. Bioeng.* **2012,** *109* (6), 1490-8.

34. Rogalski, J.; Szczodrak, J.; Pleszczyńska, M.; Fiedurek, J., Immobilisation and kinetics of Penicillium notatum dextranase on controlled porous glass. *J. Mol. Catal. B: Enzym.* **1997,** *3* (6), 271-283.

35. Xu, J.; Huo, S.; Yuan, Z.; Zhang, Y.; Xu, H.; Guo, Y.; Liang, C.; Zhuang, X., Characterization of direct cellulase immobilization with superparamagnetic nanoparticles. *Biocatal. Biotransform.* **2011,** *29* (2-3), 71-76.

36. Yang, J.; Hu, Y.; Jiang, L.; Zou, B.; Jia, R.; Huang, H., Enhancing the catalytic properties of porcine pancreatic lipase by immobilization on SBA-15 modified by functionalized ionic liquid. *Biochem. Eng. J.* **2013,** *70*, 46-54.

37. Xue, F.; Chen, Q.; Li, Y.; Liu, E.; Li, D., Immobilized lysozyme onto 1,2,3,4-butanetetracarboxylic (BTCA)-modified magnetic cellulose microsphere for improving bio-catalytic stability and activities. *Enzyme Microb. Technol.* **2019,** *131*, 109425.